Enhancement/reduction of biological pump depends on ocean circulation in the sea-ice reduction regions of the Arctic Ocean

Shigeto Nishino*

Research Institute for Global Change, Japan Agency for Marine-Earth Science and Technology, 2-15 Natsushima, Yokosuka, Kanagawa 237-0061, Japan.

Tel: +81-46-867-9487

Fax: +81-46-867-9437

nishinos@jamstec.go.jp

Takashi Kikuchi

Research Institute for Global Change, Japan Agency for Marine-Earth Science and Technology, 2-15 Natsushima, Yokosuka, Kanagawa 237-0061, Japan.

Tel: +81-46-867-9486

Fax: +81-46-867-9437

takashik@jamstec.go.jp

Michiyo Yamamoto-Kawai

Research Center for Advanced Science and Technology, Tokyo University of Marine Science and Technology, 4-5-7 Konan, Minato-ku, Tokyo 108-8477, Japan.

Tel: +81-3-5463-0735

Fax: +81-3-5463-0735

michiyo@kaiyodai.ac.jp

Yusuke Kawaguchi

Research Institute for Global Change, Japan Agency for Marine-Earth Science and Technology, 2-15 Natsushima, Yokosuka, Kanagawa 237-0061, Japan.

Tel: +81-46-867-9484

Fax: +81-46-867-9437

yusuke.kawaguchi@jamstec.go.jp

Toru Hirawake

Graduate School of Fisheries Sciences, Hokkaido University, 3-1-1 Minato-cho, Hakodate, Hokkaido 041-8611, Japan.

Tel: +81-138-40-8844

Fax: +81-138-40-5618

hirawake@salmon.fish.hokudai.ac.jp

Motoyo Itoh

Research Institute for Global Change, Japan Agency for Marine-Earth Science and Technology, 2-15 Natsushima, Yokosuka, Kanagawa 237-0061, Japan.

Tel: +81-46-867-9488

Fax: +81-46-867-9437

motoyo@jamstec.go.jp

The biological pump is a central process in the ocean carbon cycle, and is a key factor controlling atmospheric carbon dioxide (CO_2). However, whether the Arctic biological pump is enhanced or reduced by the recent loss of sea ice is still unclear. We examined if the effect was dependent on ocean circulation. Melting of sea ice can both enhance and reduce the biological pump in the Arctic Ocean, depending on ocean circulation. The biological pump is reduced within the Beaufort Gyre in the Canada Basin because freshwater accumulation within the gyre limits nutrient supply from deep layers and shelves and inhibits the growth of large-bodied phytoplankton. Conversely, the biological pump is enhanced outside the Beaufort Gyre in the western Arctic Ocean because of nutrient supply from shelves and greater light penetration, enhancing photosynthesis, caused by the sea ice loss. The biological pump could also be enhanced by sea ice loss in the Eurasian Basin, where uplifted isohaline surfaces associated with the Transpolar Drift supply nutrients upwards from deep layers. New data on nitrate uptake rates are consistent with the pattern of enhancement and reduction of the Arctic biological pump. Our estimates indicate that the enhanced biological pump can be as large as that in other oceans when the sea ice disappears. Contrary to a recent conclusion based on data from the Canada Basin alone, our study suggests that the biological CO_2 drawdown is important for the Arctic Ocean carbon sink under ice-free conditions.

Arctic Ocean circulation, Biological pump, Chlorophyll a, Nutrients, Sea ice melting

1. Introduction

In recent years, the Arctic has rapidly lost its summer sea ice cover (Comiso *et al*., 2008). The loss of sea ice increases underwater irradiance and photosynthesis and can thus enhance the biological pump in the Arctic Ocean (Nishino *et al*., 2009; Lalande *et al*., 2009). The biological pump is the mechanism by which carbon dioxide (CO_2), fixed by photosynthesis into organic matter, is transferred to deeper ocean layers as sinking particulate material, such as dead organisms and fecal pellets. As the biological pump is a key factor controlling atmospheric CO_2, enhancement of the biological pump in the Arctic Ocean contributes to regional and global carbon sinks (Bates and Mathis, 2009) and may counteract ocean acidification caused by increased atmospheric CO_2 and sea ice melt (Yamamoto-Kawai *et al*., 2009). However, freshwater inputs from melting sea ice to the surface layer strengthens water column stratification and may inhibit nutrient supply from deep layers to the surface layer, in turn affecting phytoplankton growth (Li *et al*., 2009; Cai *et al*., 2010). In fact, average phytoplankton size in the Canada Basin decreased between 2004 and 2008 (Li *et al*., 2009), implying a decrease in the efficiency of the biological pump. Thus, the overall impact of sea ice melt on the Arctic biological pump is still unclear.

Recently, McLaughlin and Carmack (2010) indicated that the nutricline, the layer where nutrient concentrations increase rapidly with depth, became deeper in the Canada Basin from 2003 to 2009, and that this deepening was caused by an accumulation of surface freshwater within the Beaufort Gyre associated with sea ice melt. Therefore, ocean circulation seems to play an important role in the changes of nutrient distribution and biological activities. Here we extend their study to regions outside the Beaufort Gyre to examine

responses of the biological pump to the sea ice melt in different Arctic Ocean basins with different circulation patterns.

2. Data and Methods

We conducted hydrographic surveys over the Chukchi Sea shelf and Canadian Basin (Canada Basin and Makarov Basin) in the western Arctic Ocean during the summer of 2008/2009 (August–October) using the R/V *Mirai* of the Japan Agency for Marine-Earth Science and Technology (JAMSTEC). The observed results were compared with those obtained during cruises of the R/V *Mirai* in 2002, the USCGC *Polar Star* in 2002 (Woodgate *et al*., 2002), the CCGS *Louis S. St-Laurent* in 2003 (McLaughlin *et al*., 2010), and the Arctic Ocean Section in 1994 (AOS94) (Wheeler, 1997). Locations of the hydrographic stations are shown in Fig. 1.

General descriptions of the R/V *Mirai* cruises in 2002, 2008, and 2009 are presented in the cruise reports (Shimada, 2002, 2008; Kikuchi, 2009), and the data can be downloaded from the JAMSTEC Data Site for Research Cruises (http://www.godac.jamstec.go.jp/cruisedata/mirai/e/index.html). A conductivity-temperature-depth system (CTD; Sea-Bird Electronics Inc., SBE9plus) and a Carousel water sampling system with 36 Niskin bottles (12 L) were used for the observations. Seawater samples were collected for measurements of salinity, dissolved oxygen, nutrients (nitrate, nitrite, phosphate, silicate, and ammonium), total and size-fractionated chlorophyll *a*, biological uptake rates of nitrogen (only in 2009), and other chemical and biological parameters. Bottle salinity samples were analyzed following the GO-SHIP (Global Ocean Ship-based Hydrographic Investigations Program) Repeat Hydrography Manual (Hydes *et al*., 2010) using a Guildline AUTOSAL salinometer and IAPSO (International Association for the

Physical Sciences of the Oceans) standard seawater as a reference material (Kawano, 2010). Dissolved oxygen samples were measured by Winkler titration following the WHP (World Ocean Circulation Experiment Hydrographic Program) operations and methods (Dickson, 1996). Nutrient samples were analyzed according to the GO-SHIP Repeat Hydrography Manual (Hydes *et al*., 2010) using reference materials of nutrients in seawater (Aoyama and Hydes, 2010; Sato *et al*., 2010) except for the 2002 R/V *Mirai* cruise. Chlorophyll *a* in seawater samples was measured using a fluorometric non-acidification method (Welschmeyer, 1994) and a Turner Design fluorometer (10-AU-005). For size-fractionated chlorophyll *a* measurements, phytoplankton cells in the water samples were fractionated using three types of nucleopore filters (pore sizes: 10, 5, and 2 μm) and a Whatman GF/F filter (pore size: ~0.7 μm). Nitrogen uptake rates were measured on the 2009 R/V *Mirai* cruise under simulated *in situ* incubation conditions, which were similar to those of Lee and Whitledge (2005).

The data from the USCGC *Polar Star* cruise in 2002 were downloaded from the website of Chukchi Borderland, Polar Science Center, Applied Physics Laboratory, University of Washington (http://psc.apl.washington.edu/CBL.html). The data of the CCGS *Louis S. St-Laurent* cruise in 2003 were downloaded from the website of Beaufort Gyre Exploration Project, Woods Hole Oceanographic Institution (http://www.whoi.edu/beaufortgyre/data.html). We also downloaded the AOS94 data from the Oceanographic Data Facility, Scripps Institution of Oceanography (http://sts.ucsd.edu/sts/odf).

Historical data were also used to extend our investigation to include the eastern Arctic Ocean. Hydrographic data (temperature and salinity) were obtained from the Atlas of the Arctic Ocean created by the Environmental Working Group (Arctic Climatology Project, 1998). Nutrient data were obtained from the

Hydrochemical Atlas of the Arctic Ocean (Colony and Timokhov, 2001). These data were provided on CD-ROMs.

3. Results

A dramatic change was detected in the distribution of large-bodied phytoplankton (>10 μm): Chlorophyll *a* (Chl-*a*) of large-bodied phytoplankton was found in both the Chukchi Sea shelf and Canada Basin in 2002/2003, but it had a very low concentration in the Canada Basin in 2008/2009 (Fig. 2a and 2b). Chlorophyll *a* of small-bodied phytoplankton (<10 μm) also decreased from 2002/2003 to 2008/2009 at its vertical maximum concentration, at around a 50 m depth, in the Canada Basin, but its Chl-*a* maximum still appeared in 2008/2009 (Fig. 2c and 2d). In contrast, in the Chukchi Sea shelf, Chl-*a* of small-bodied phytoplankton increased from 2002/2003 to 2008/2009 over the whole of the water column. Li *et al*. (2009) explained that the decrease in large-bodied phytoplankton in the Canada Basin was caused by a decrease in nutrients in the euphotic zone, which was a result of enhanced stratification due to sea ice melt. However, the nutrient decrease in the euphotic zone would not greatly influence the growth of small-bodied phytoplankton because they have a large surface-area-to-volume ratio that provides effective acquisition of nutrients. This is shown by the appearance of the small-bodied phytoplankton Chl-*a* maximum, and the disappearance of the large-bodied phytoplankton Chl-*a* maximum in 2008/2009. The increase in small-bodied phytoplankton in the shelf area might be related to the recent warming of shelf seas, although there is a range of other potential explanatory factors.

Because the detritus of large cells effectively transports organic carbon to deeper layers (Michaels and Silver, 1988), the disappearance of large-bodied

phytoplankton implies a reduction of the efficiency of the biological pump in the Canada Basin. We also found that the nitrate uptake rate by phytoplankton, which is assumed to be in balance with the flux of sinking particles associated with the biological pump, actually decreased from 0.25 mg-N/m^2/h in 2002 (Lee and Whitledge, 2005) to 0.08 mg-N/m^2/h in 2009 (averages of three stations indicated by yellow circles in Fig. 2f and yellow profiles in Fig. 3) in the Canada Basin. This decrease can be explained by decreased nutrient availability, as shown in distributions of nitrate, which is the limiting nutrient of Arctic phytoplankton production (Tremblay and Gagnon, 2009), at a depth of 50 m (Fig. 2e and 2f). The depth of 50 m roughly corresponds to the bottom of the euphotic zone and the Chl-*a* maximum layer (Nishino *et al*., 2008; McLaughlin and Carmack, 2010). At this depth, nitrate decreased from 2002/2003 to 2008/2009 in the Canada Basin, which in turn would have decreased the nitrate uptake by phytoplankton and the efficiency of the biological pump.

In contrast to the Canada Basin, nitrate concentrations at 50 m depth in the Makarov Basin, where observations were conducted only in 2002 and 2008, were higher in 2008 than in 2002. This is because the nutricline shallowed, from 25–30 m in 2002 to approximately 10 m in 2008, accompanied by a shoaling of isohaline surfaces around a salinity of approximately 31 (Fig. 4). To examine the effect of ocean circulation on nitrate distribution, we evaluated dynamic heights, which represent geostrophic flow fields, at 50 m compared to those at 250 m, where ocean currents were assumed to be slow. The dynamic heights at 50 m in the overall study area were calculated from the temperature and salinity data collected in 2002/2003 and 2008/2009, and the circulation patterns were overlaid on the nitrate distributions as shown in Fig. 2e and 2f, respectively. The dynamic heights clearly suggest that the change in nitrate was associated with a change in ocean

circulation. The shoaling of isohaline surfaces in the Makarov Basin was geostrophically associated with strong northward flows north of the Chukchi Sea shelf that were found in 2008/2009 (Fig. 2f) and carry nutrient-rich shelf water into the basin. Thus, in this region, where nutrients were sufficiently supplied, light conditions could be the limiting factor of phytoplankton production, and hence sea ice melt should increase production.

Our observation area in the Makarov Basin was covered by sea ice in 2002, whereas it was open water in 2008. Because we do not have Chl-*a* data for the Makarov Basin, we instead compared the near-bottom nitrate concentrations along almost identical sections examined in 2002 and 2008 (Fig. 5). In both 2002 and 2008, nitrate concentrations increased near the bottom of the water column while oxygen levels decreased, which suggested that there was the decomposition of organic matter on the seabed. The increase in nitrate concentrations near the bottom of the water column was greater in 2008 than in 2002. This implies that the deposition of organic matter on the bottom increased from 2002 to 2008, which was most likely due to the enhanced biological pump.

Comparison of nitrate profiles at a station located between the Canada and Makarov basins (red circle in Fig. 2f) obtained in 1994 under the sea ice cover (Wheeler, 1997) with those obtained in 2009 in open water also showed a recent increase in near-bottom nitrate concentrations (Fig. 6). This suggested an increase in the organic matter deposition with the sea ice melt. We measured nitrate uptake rates in 2009 at this station, where the subsurface (50-m depth) nitrate concentrations were relatively high compared with those in the interior of Canada Basin (Fig. 2f). The nitrate uptake rate had its vertical maximum around the depth of the Chl-*a* maximum concentration of large-bodied phytoplankton of > 10 μm (red profiles in Fig. 3). The rates at this station were much higher than those

measured in the nitrate-poor Canada Basin (yellow circles in Fig. 2f and yellow profiles in Fig. 3). The higher rates seemed to result from higher Chl-*a* concentrations of large-bodied phytoplankton over the whole of the water column.

4. Discussion

The anticyclonic circulation in the Canada Basin, called the Beaufort Gyre, increased in strength and latitudinal width from 2002/2003 to 2008/2009 (Fig. 2e and 2f). Arctic Ocean circulation, and especially the Beaufort Gyre, has recently become enhanced because the melting of thick, solid multi-year ice has produced fragmented and mobile sea ice, which allows the wind to more efficiently drive the ocean circulation (Shimada *et al*., 2006; Yang, 2009). As surface freshwater (including that from melting sea ice) has accumulated in the Beaufort Gyre, by the convergence of Ekman transport, the freshwater content of the Canada Basin has gradually increased with the enhanced ocean circulation observed from 2003 to 2007 (Proshutinsky *et al*., 2009). The accumulation of fresh and nutrient-poor surface waters can inhibit nutrient supply from deep layers and thus decrease phytoplankton production (McLaughlin and Carmack, 2010).

Consideration of the effects of ocean circulation should be expanded from the above vertical one-dimensional interpretation. The accumulation of freshwater within the Beaufort Gyre produces a density gradient between the shelf and basin, resulting in the formation of a strong westward flow over the shelf slope, as shown by the dynamic height in 2008/2009 (Fig. 2f). This strong westward flow prevented the spread of nutrient-rich shelf waters towards the central Canada Basin in 2008/2009, which inhibited phytoplankton growth and reduced the efficiency of the biological pump in the Canada Basin (Fig. 2b). In contrast, in 2002/2003 a weak density gradient and a weak westward flow between the shelf

and basin should have allowed nutrient-rich shelf water to spread into the basin (Fig. 2e). In addition, a pathway for nutrient-rich water to move from the Siberian shelf into the Canada Basin, north of the narrow Beaufort Gyre (north of 76°N and east of 160°W), appeared in 2002/2003. These nutrient supplies in 2002/2003 resulted in a flourishing phytoplankton population, even in the Canada Basin (Fig. 2a). Thus, the biological pump decreases within the Beaufort Gyre where freshwater accumulates because of the stronger ocean circulation in the fragmented and mobile sea ice conditions that follow sea ice melt.

Outside the Beaufort Gyre, nitrate concentrations at 50 m depth were higher than those inside the gyre (Fig. 2e and 2f) because of the weaker influence of nutrient-poor freshwater. The sufficient nutrient conditions outside the gyre should increase the efficiency of the biological pump with the sea ice melt as shown by the increases in near-bottom nitrate concentrations (Figs. 5 and 6). The nitrate uptake rate integrated over the water column at the station between the Canada and Makarov basins (red circle in Fig. 2f and the red profile in Fig. 3) was 0.42 mg-N/m^2/h. This rate is close to the global mean of particulate organic nitrogen export from the surface ocean (0.58 mg-N/m^2/h), calculated from the global mean of particulate organic carbon export (Dunne *et al*., 2005) and a stoichiometric ratio of carbon and nitrogen (Redfield *et al*., 1963). Therefore, if there is a sufficient nutrient, the biological pump can be as large as that in other oceans when the sea ice disappears.

Nutrient availability for phytoplankton production in the Makarov Basin would increase because of a shoaling of nutricline with a shoaling of isohaline surfaces around a salinity of approximately 31 (Fig. 4). Here we propose a mechanism for the shoaling of nutricline and isohaline surfaces. In 2008, a larger volume of nutrient-rich water with a salinity of 32–33 occupied the Makarov

Basin (Fig. 4b) compared with that in 2002 (Fig. 4a), resulting in the shoaling of isohaline surfaces above it. This large-volume of water with a salinity of 32–33 found in 2008 was also characterized by a temperature minimum of near-freezing temperatures (Fig. 7b). In the Makarov Basin, the nutrient-rich water seems to be supplied from the East Siberian Sea (Fig. 2f). These features suggest that the temperature minimum was caused by cooling and convection in the East Siberian Sea and the water mass was then carried northward, along with the high nutrient concentrations from remineralization at the shelf bottom of the East Siberian Sea, into the Makarov Basin. The formation of such a water mass in the East Siberian Sea has become more likely in recent years because of the significant delays in autumn freeze-up (Markus *et al*., 2009). The delay in freezing results in an increased duration of water mass formation by cooling and convection because sea ice cover prevents atmospheric cooling and mixing by wind. The extensive temperature minimum found in 2008 compared with that in 2002 (Fig. 7) strongly suggests a recent increase in the volume of water that has been formed by the previously described process. Conversely, the temperature maximum water with a salinity of 32.5–33 found in 2002 suggests that the water was not subjected to the sufficient cooling and convection over the shelf during winter. Consequently, the shoaling of nutricline was likely caused by the input of the large-volume water mass with low temperature and high nutrients formed in the East Siberian Sea during winter.

In the Eurasian Basin of the eastern Arctic Ocean (Amundsen Basin and Nansen Basin), sea ice still covers the ocean even in summer, and therefore we do not have data to examine biogeochemical changes associated with sea ice disappearance in this basin. Here we propose a conceivable scenario, from the viewpoint of ocean circulation, using historical data sets (Arctic Climatology

Project, 1998; Colony and Timokhov, 2001). Ocean circulation in the Eurasian Basin is characterized by the Transpolar Drift flowing from the Siberian shelves to the Fram Strait. The Transpolar Drift accompanies a shoaling of isohaline surfaces from the Canadian Basin towards the Eurasian Basin (Fig. 8a and 8b). Because of the shoaling of isohaline surfaces, surface nitrate concentrations in the Eurasian Basin are relatively high compared with those in the Canadian Basin (Fig. 8c). Therefore, if sea ice were to disappear from the Eurasian Basin, a marked increase in phytoplankton production could occur. However, surface silicate concentrations in the Eurasian Basin are extremely low (Fig. 8d), and only weakly affected by high-silicate waters of Pacific origin (Jones and Anderson, 1986). Assuming that diatoms exhaust the surface silicate content (5 μmol/l) over the 120-day growth season (Subba Rao and Platt, 1984) in the ice-free Eurasian Basin, that silicate uptake linearly decreases with depth to be zero at 50 m, and that nitrate uptake by diatoms occurs with a Si:N ratio of 1:1 (Brzezinski, 1985), the nitrate uptake rate is estimated as 0.61 mg-N/m^2/h. This value is similar to that observed outside the Beaufort Gyre in the Canadian Basin of the western Arctic Ocean (0.42 mg-N/m^2/h) and much higher than that within the Beaufort Gyre (0.08 mg-N/m^2/h) observed in 2009. When the nitrate uptake rate is converted to the carbon uptake rate using a stoichiometric C:N ratio of 106:16 (Redfield *et al.*, 1963), the annual rate over the Eurasian Basin (1.5×10^6 km^2) is estimated as 15 TgC/yr. Although this estimation of the rate is based on assumptions with large uncertainties, it corresponds to 7.5–23% of the present Arctic Ocean carbon sink of approximately 66–199 TgC/yr (Bates and Mathis, 2009). A recent study using data from the Canada Basin concluded that the Arctic Ocean basin will not become a large sink of CO_2 because of strong surface stratification and low biological productivity (Cai *et al*., 2010). However, our study suggests that this is

not the case for the region outside the Beaufort Gyre, and that biological CO_2 drawdown is indeed important for the Arctic Ocean carbon sink under ice-free conditions.

The historical data sets described above (Arctic Climatology Project, 1998; Colony and Timokhov, 2001) are compilations of previously reported data before 2000. It would be informative to compare them with recent data after 2000. During summer 2005, the Swedish icebreaker *Oden* crossed the Arctic Ocean from north of Barrow, Alaska, to Svalbard. The water mass and nutrient distributions obtained from the *Oden* cruise (Jones *et al*., 2008) were basically similar to those from the historical data. However, upper ocean salinity in 2005 was lower than that of the historical data. The decrease in salinity in the Eurasian Basin could be explained by an increase in river water inventories (Jones *et al*., 2008), which would be associated with a change of wind patterns over the Siberian shelve seas (Johnson and Polyakov, 2001; Boyd *et al*., 2002). Nitrate and silicate concentrations in the upper ocean of the Eurasian Basin in 2005 were also lower than those of the historical data. During summer 2005, heavy sea ice covered the Eurasian Basin, and therefore the nutrient decreases could not be explained by the biological uptake of nutrients but instead may have resulted from upper ocean freshening by river water influences. If the sea ice were to disappear from the Eurasian Basin, the river water influences might negatively affect the biological productivity, but the shallower nutricline and higher nitrate concentrations in the upper ocean compared to those in the Canadian Basin could increase the biological productivity in the Eurasian Basin.

5. Conclusions and Implications

The biological pump is reduced within the Beaufort Gyre and enhanced outside the gyre with the loss of sea ice (Fig. 9). The Makarov and Eurasian basins, where few previous observations have been made, lie outside the Beaufort Gyre and are key areas for future study if we are to understand changes in the behavior of biogeochemical cycles in response to melting sea ice. Furthermore, because Arctic waters flow through the channels of the Canadian Archipelago and Fram Strait, transporting nutrients to the North Atlantic (Jones *et al*., 2003), changes in nutrient use and the biological pump in the Arctic Ocean might affect biological productivity in the North Atlantic.

Acknowledgments. We thank K. Shimada, the chief scientist of the R/V *Mirai* cruises in 2002 and 2008, and the captain, officers, and crew of the R/V *Mirai*, which was operated by Global Ocean Development, Inc. We also thank the staff of Marine Works Japan, Ltd. for their skillful work aboard the ship and with data processing. Geographical maps and figures were illustrated using Ocean Data View software (Schlitzer, 2006).

References

Aoyama, M. and D. J. Hydes (2010): How do we improve the comparability of nutrient measurements? p. 1-10. In *Comparability of nutrients in the world's ocean*, ed. by M. Aoyama, A. G. Dickson, D. J. Hydes, A. Murata, J. R. Oh, P. Roose and E. M. S. Woodward, Mother Tank, Tsukuba, Japan.

Arctic Climatology Project (1998): *Environmental Working Group Joint U.S.-Russian Atlas of the Arctic Ocean - summer period*, ed. by L. Timokhov and F. Tanis, Environmental Research Institute of Michigan in association with the National Snow and Ice Data Center, Ann Arbor, Michigan, U.S.A., CD-ROM.

Bates, N. R. and J. T. Mathis (2009): The Arctic Ocean marine carbon cycle: Evaluation of air-sea CO_2 exchanges, ocean acidification impacts and potential feedbacks. *Biogeosciences*, **6**, 2433-2459.

Boyd, T. J., M. Steele, R. D. Muench and J. T. Gunn (2002): Partial recovery of the Arctic Ocean halocline. *Geophys*. *Res*. *Lett*., **29**, 1657, doi:10.1029/2001GL014047.

Brzezinski, M. A. (1985): The Si:C:N ratio of marine diatoms: Interspecific variability and the effect of some environmental variables. *J*. *Phycol*., **21**, 347-357.

Cai, W.-J., L. Chen, B. Chen, Z. Gao, S. H. Lee, J. Chen, D. Pierrot, K. Sullivan, Y. Wang, X. Hu, W.-J. Huang, Y. Zhang, S. Xu, A. Murata, J. M. Grebmeier, E. P. Jones and H. Zhang

(2010): Decrease in the CO_2 uptake capacity in an ice-free Arctic Ocean basin. *Science*, doi: 10.1126/science.1189338.

Colony, R. and L. Timokhov (2001): *Hydrochemical Atlas of the Arctic Ocean*. International Arctic Research Center, University of Alaska, Fairbanks, U.S.A., and State Research Center – the Arctic and Antarctic Research Institute, St. Petersburg, Russia, CD-ROM.

Comiso, J. C., C. L. Parkinson, R. Gersten and L. Stock (2008): Accelerated decline in the Arctic sea ice cover. *Geophys*. *Res*. *Lett*., **35**, L01703, doi:10.1029/2007GL031972.

Dickson, A. G. (1996): Determination of dissolved oxygen in sea water by Winkler titration, In *WOCE Operations Manual*, Volume 3, Section3.1, Part 3.1.3 WHP Operations and Methods, WHP Office Report WHPO 91-1, WOCE Report No. 68/91, Nov. 1994, Revision 1, Woods Hole, Massachusetts, U.S.A., 13 pp.

Dunne, J. P., R. A. Armstrong, A. Gnanadesikan and J. L. Sarmiento (2005): Empirical and mechanistic models for the particle export ratio. *Global Biogeochem*. *Cycles*, **19**, GB4026, doi:10.1029/2004GB002390.

Hydes, D. J., M. Aoyama, A. Aminot, K. Bakker, S. Becker, S. Coverly, A. Daniel, A. G. Dickson, O. Grosso, R. Kerouel, J. van Ooijen, K. Sato, T. Tanhua, E. M. S. Woodward and J. Z. Zhang (2010): Determination of dissolved nutrients (N, P, Si) in seawater with high precision and inter-comparability using das-segmented continuous flow analysers. In *The GO-SHIP Repeat Hydrography Manual: A Collection of Expert Reports and Guidelines*, IOCCP Report Number 14, ICPO Publication Series Number 134, ed. by E. M. Hood, C. L. Sabine and B. M. Sloyan, UNESCO-IOC, Paris, France, www.go-ship.org/HydroMan.html.

Johnson, M. A. and I. V. Polyakov (2001): The Laptev Sea as a source for recent Arctic Ocean salinity changes. *Geophys*. *Res*. *Lett*., **28**, 2017-2020.

Jones, E. P. and L. G. Anderson (1986): On the origin of the chemical properties of the Arctic Ocean halocline. *J. Geophys*. *Res*., **91**, 10,759-10,767.

Jones, E. P., L. G. Anderson, S. Jutterström, L. Mintrop and J. H. Swift (2008): Pacific freshwater, river water and sea ice meltwater across Arctic Ocean basins: Results from the 2005 Beringia Expedition. *J. Geophys*. *Res*., **113**, C08012, doi:10.1029/2007JC004124.

Jones, E. P., J. H. Swift, L. G. Anderson, M. Lipizer, G. Civitarese, K. K. Falkner, G. Kattner and F. McLaughlin (2003): Tracing Pacific water in the North Atlantic Ocean. *J. Geophys*. *Res*., **108**, 3116, doi:10.1029/2001JC001141.

Kawano, T. (2010): Method for salinity (conductivity ratio) measurement. In *The GO-SHIP Repeat Hydrography Manual: A Collection of Expert Reports and Guidelines*, IOCCP Report Number 14, ICPO Publication Series Number 134, ed. by E. M. Hood, C. L. Sabine and B. M. Sloyan, UNESCO-IOC, Paris, France, www.go-ship.org/HydroMan.html.

Kikuchi, T. (2009): *R/V Mirai Cruise Report MR09-03*. JAMSTEC, Yokosuka, Japan, 190 pp.

Lalande, C., S. Bélanger and L. Fortier (2009): Impact of a decreasing sea ice cover on the vertical export of particulate organic carbon in the northern Laptev Sea, Siberian Arctic Ocean. *Geophys. Res*. *Lett*., **36**, L21604, doi:10.1029/2009GL040570.

Lee, S. H. and T. E. Whitledge (2005): Primary and new production in the deep Canada Basin during summer 2002. *Polar Biol*., **28**, 190–197.

Li, W. K. W., F. A. McLaughlin, C. Lovejoy and E. C. Carmack (2009): Smallest algae thrive as the Arctic Ocean freshens. *Science*, **326**, 539.

Markus, T., J. C. Stroeve and J. Miller (2009): Recent changes in Arctic sea ice melt onset, freezeup, and melt season length. *J. Geophys. Res*., **114**, C12024, doi:10.1029/2009JC005436.

McLaughlin, F. A. and E. C. Carmack (2010): Deepening of the nutricline and chlorophyll maximum in the Canada Basin interior, 2003-2009. *Geophys. Res. Lett*., **37**, L24602, doi:10.1029/2010GL045459.

McLaughlin, F. A., A. Proshutinsky, E. C. Carmack, K. Shimada, M. Corkum, V. Forsland, C. Guay, C. Guéguen, B. van Hardenberg, R. Hopcroft, M. Itoh, R. Krishfield, L. Miller, J. Nelson, W. Richardson, D. Sieberg, J. Smith, M. Steel, N. Tanaka, L. White and S. Zimmermann (2010): *Physical, chemical and zooplankton data from the Canada Basin, August 2003*. Canadian data report of hydrography and ocean sciences 184, Fisheries and Oceans, Science Branch, Pacific Region, Institute of Ocean Sciences, Sidney, British Columbia, Canada, 303 pp.

Michaels, A. F. and M. W. Silver (1988): Primary production, sinking fluxes and the microbial food web. *Deep-Sea Res*., **35**, 473-490.

National Ice Center (2006): *National Ice Center Arctic Sea ice charts and climatologies in gridded format*, ed. by F. Fetterer and C. Fowler, National Snow and Ice Data Center, Boulder, Colorado, U.S.A.

Nishino, S., K. Shimada, M. Itoh and S. Chiba (2009): Vertical double silicate maxima in the sea-ice reduction region of the western Arctic Ocean: Implications for an enhanced biological pump due to sea-ice reduction. *J. Oceanogr*., **65**, 871-883, doi:10.1007/s10872-009-0072-2.

Nishino, S., K. Shimada, M. Itoh, M. Yamamoto-Kawai and S. Chiba (2008): East-west differences in water mass, nutrient, and chlorophyll *a* distributions in the sea-ice reduction region of the western Arctic Ocean. *J. Geophys. Res*., **113**, C00A01, doi:10.1029/2007JC004666.

Proshutinsky, A., R. Krishfield, M.-L. Timmermans, J. Toole, E. Carmack, F. McLaughlin, W. J. Williams, S. Zimmermann, M. Itoh and K. Shimada (2009): Beaufort Gyre freshwater reservoir: State and variability from observations. *J. Geophys. Res*., **114**, C00A10, doi:10.1029/2008JC005104.

Redfield, A. C., B. H. Ketchum and F. A. Richards (1963): The influence of organisms on the composition of seawater. p. 26-77. In *The Sea* Vol. 2, ed. by M. N. Hill, Wiley, New York, U.S.A.

Sato, K., M. Aoyama and S. Becker (2010): Reference materials for nutrients in seawater as calibration standard solution to keep comparability for several cruises in the world ocean in 2000s. p. 43-56. In *Comparability of nutrients in the world's ocean*, ed. by M. Aoyama, A.

G. Dickson, D. J. Hydes, A. Murata, J. R. Oh, P. Roose and E. M. S. Woodward, Mother Tank, Tsukuba, Japan.

Schlitzer, R. (2006): *Ocean Data View*. http://odv.awi.de.

Shimada, K. (2002): *R/V Mirai Cruise Report MR02-K05 Leg1*. JAMSTEC, Yokosuka, Japan, 226 pp.

Shimada, K. (2008): *R/V Mirai Cruise Report MR08-04 (R/V Mirai International Polar Year 2008 cruise)*. JAMSTEC, Yokosuka, Japan, 163 pp.

Shimada, K., T. Kamoshida, M. Itoh, S. Nishino, E. Carmack, F. McLaughlin, S. Zimmermann and A. Proshutinsky (2006): Pacific Ocean inflow: influence on catastrophic reduction of sea ice cover in the Arctic Ocean. *Geophys*. *Res*. *Lett*., **33**, L08605, doi:10.1029/2005GL025624.

Subba Rao, D. V. and T. Platt (1984): Primary production of Arctic waters. *Polar Biol*., **3**, 191-210.

Tremblay, J.-É. and J. Gagnon (2009): The effects of irradiance and nutrient supply on the productivity of Arctic waters: a perspective on climate change. p. 73-92. In *Influence of Climate Change on the Changing Arctic and Sub-Arctic Conditions*, ed. by J. C. J. Nihoul and A. G. Kostianoy, Springer, Dordrecht, Netherlands.

Welschmeyer, N. A. (1994): Fluorometric analysis of chlorophyll *a* in the presence of chlorophyll *b* and pheopigments. *Limnol*. *Oceanogr*., **39**, 1985–1992.

Wheeler, P. A. (1997): Preface: the 1994 Arctic Ocean Section. *Deep-Sea Res*. *II*, **44**, 1483–1485.

Woodgate, R. A., K. Aagaard, J. H. Swift, W. M. Smethie and K. K. Falkner (2002): *Chukchi Borderland Cruise CBL2002 Arctic West - Phase II (AWS-02-II)*. University of Washington, Seattle, Washington, U.S.A., 51 pp.

Yamamoto-Kawai, M., F. McLaughlin, E. Carmack, S. Nishino and K. Shimada (2009): Aragonite undersaturation in the Arctic Ocean: Effects of ocean acidification and sea ice melt. *Science*, **326**, 1098-1100.

Yang, J. (2009): Seasonal and interannual variability of downwelling in the Beaufort Sea. *J. Geophys*. *Res*., **114**, C00A14, doi:10.1029/2008JC005084.

Figure Legends

Fig. 1. Map showing bathymetric features of the study area and locations of the hydrographic stations of the R/V *Mirai* Arctic Ocean Cruises in 2002 (blue), 2008 (yellow), and 2009 (red), and the Chukchi Borderland Cruise by the USCGC *Polar Star* in 2002 (dark green) (Woodgate *et al*., 2002), and the cruise of the CCGS *Louis S. St-Laurent* in 2003 (lime green) (McLaughlin *et al*., 2010). Open circles indicate CTD and hydrographic water sampling stations; closed circles indicate CTD observation stations. Geographical locations are abbreviated as follows: Canada Basin (CB), Northwind Ridge (NWR), Chukchi Plateau (CP), Chukchi Abyssal Plain (ChuAP), Mendeleyev Ridge (MR), and Makarov Basin (MB).

Fig. 2. Vertical sections of phytoplankton chlorophyll *a* [μg/L] in large-sized cells of > 10 μm (colors) and salinity (contours) in (a) 2002/2003 and (b) 2008/2009, vertical sections of

phytoplankton chlorophyll *a* [μg/L] in small size cells of < 10 μm (colors) and salinity (contours) in (c) 2002/2003 and (d) 2008/2009, and dynamic height [dyn m] at 50 m relative to 250 db (dashed contours) and nitrate [μmol/kg] at 50 m (colors) in (e) 2002/2003 and (f) 2008/2009. The sections in (a) – (d) are illustrated along red lines in (e) and (f). The blue lines in (e) and (f) show the sections of nitrate distributions in Figs. 4 and 5. Red and yellow circles in (f) indicate stations where nitrate uptake rates were measured in 2009 (Fig. 3). Data were obtained from cruises by the R/V *Mirai* in 2002, 2008, and 2009, USCGC *Polar Star* in 2002 (Woodgate *et al*., 2002), and CCGS *Louis S. St-Laurent* in 2003 (McLaughlin *et al*., 2010).

Fig. 3. Vertical profiles of (a) nitrate uptake rate [mg-N/m^3/h] and (b) phytoplankton chlorophyll *a* [μg/L] in large-sized cells of > 10 μm at stations indicated by red and yellow circles in Fig 2f. The profiles at red and yellow circle stations are represented by red and yellow lines, respectively. In (a), the nitrate uptake rates integrated over the water columns at red and yellow circle stations are 0.42 and 0.08 [mg-N/m^2/h], respectively. The integrated rate at yellow circle stations is an average of three stations. Data are from the R/V *Mirai* in 2009.

Fig. 4. Vertical sections of nitrate (colors) [μmol/kg] and salinity (contours) from the sea surface to 200 m in the Makarov Basin observed in (a) 2002 and (b) 2008 along the blue lines in Fig. 2e and 2f, respectively. Data are from the USCGC *Polar Star* in 2002 (Woodgate *et al*., 2002) and R/V *Mirai* in 2008.

Fig. 5. Vertical sections of nitrate [μmol/kg] from the sea surface to seafloor in the Makarov Basin observed in (a) 2002 and (b) 2008 along the blue lines in Fig. 2e and 2f, respectively. Data are from the USCGC *Polar Star* in 2002 (Woodgate *et al*., 2002) and R/V *Mirai* in 2008.

Fig 6. Monthly sea ice concentrations (white = 100 %, blue = 0 %) in September of (a) 1994 and (b) 2009 (National Ice Center, 2006), and (c) vertical profiles of nitrate obtained from the Arctic Ocean Section cruise in 1994 (Wheeler, 1997) depicted by open circles (○) and the R/V *Mirai* cruise in 2009 shown by open squares (□). The positions where the profiles were obtained are almost the same and indicated by dots in (a) and (b), respectively. The position in 2009 is equivalent to the red circle in Fig. 2f.

Fig. 7. Vertical sections of temperature (colors) [deg. C] and salinity (contours) from the sea surface to 200 m in the Makarov Basin observed in (a) 2002 and (b) 2008 along the blue lines in Fig. 2e and 2f, respectively. Data are from the USCGC *Polar Star* in 2002 (Woodgate *et al*., 2002) and R/V *Mirai* in 2008.

Fig. 8. (a) Map of the Arctic Ocean and pan-Arctic sections showing (b) salinity, (c) nitrate [μmol/l], and (d) silicate [μmol/l]. Geographical locations are abbreviated as follows: Canada Basin (CB), Mendeleyev Ridge (MR), Makarov Basin (MB), Lomonosov Ridge (LR), Amundsen Basin (AB), Arctic Mid-Ocean Ridge (AMOR), and Nansen Basin (NB). Data were obtained from

the Environmental Working Group Atlas of the Arctic Ocean (Arctic Climatology Project, 1998) and Hydrochemical Atlas of the Arctic Ocean (Colony and Timokhov, 2001).

Fig. 9. Summary of the responses of ocean circulation, nutrient supply, and phytoplankton distribution to the recent Arctic sea ice loss. The Beaufort High (blue arrows), which is a high pressure over the Canada Basin of the Arctic Ocean, drives the sea ice and ocean anticyclonically as the Beaufort Gyre (BG). Sea ice loss, for example from 2002/2003 (left panel) to 2008/2009 (right panel), enhances the ocean circulation by increasing the Ekman pumping (w_e). This results in a deepening nutricline (depicted by the boundary between layers colored by light blue and red). Moreover, an enhanced westward flow between the shelf and basin areas (shown by the red cylinder in the right panel) prevents the spreading of nutrient-rich shelf water into the BG. The increase in the latitudinal width of the BG also inhibits the nutrient supply from the East Siberian Sea (ESS). The shutdown of nutrient supply from the shelves and deep layers suppresses phytoplankton growth within the BG. However, the enhanced westward flow carrying nutrient-rich shelf water turns to the north outside the BG and supplies nutrients there. In addition, significant delays in autumn freeze-up in ESS increase the supply of water with low temperature and high nutrients from ESS to the Makarov Basin outside the BG. Due to these nutrient supplies, phytoplankton growth increases outside the BG if the sea ice disappears and the underwater irradiance increases.

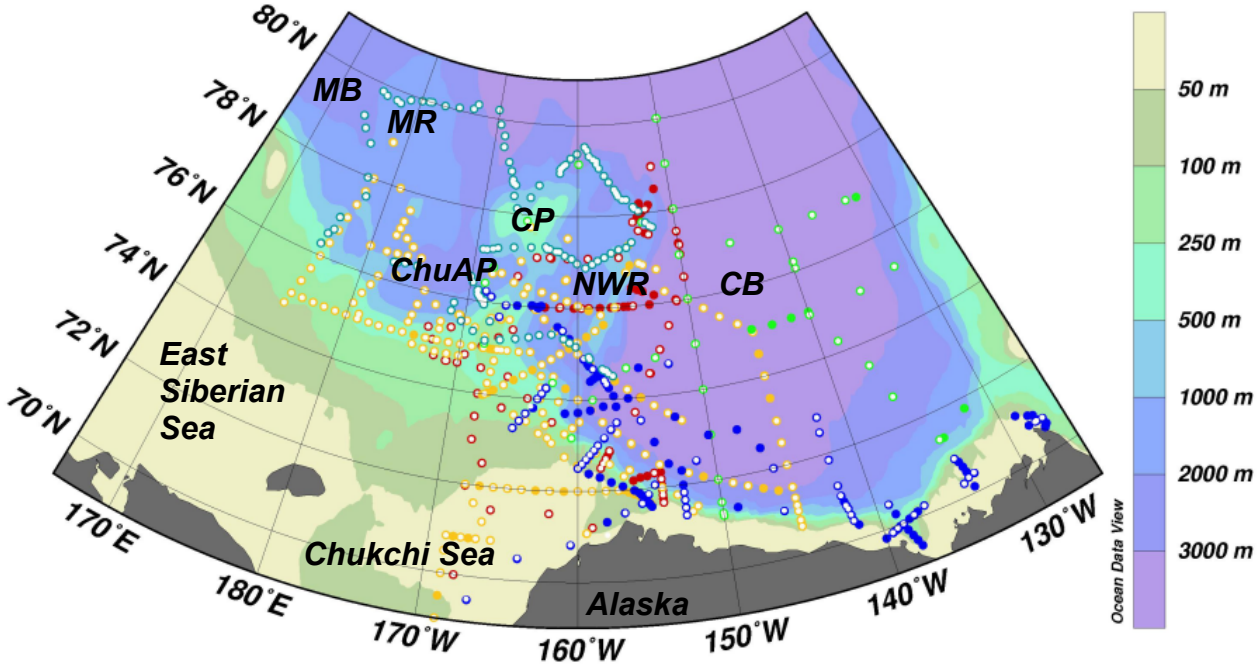

Fig. 1. Nishino *et al*.

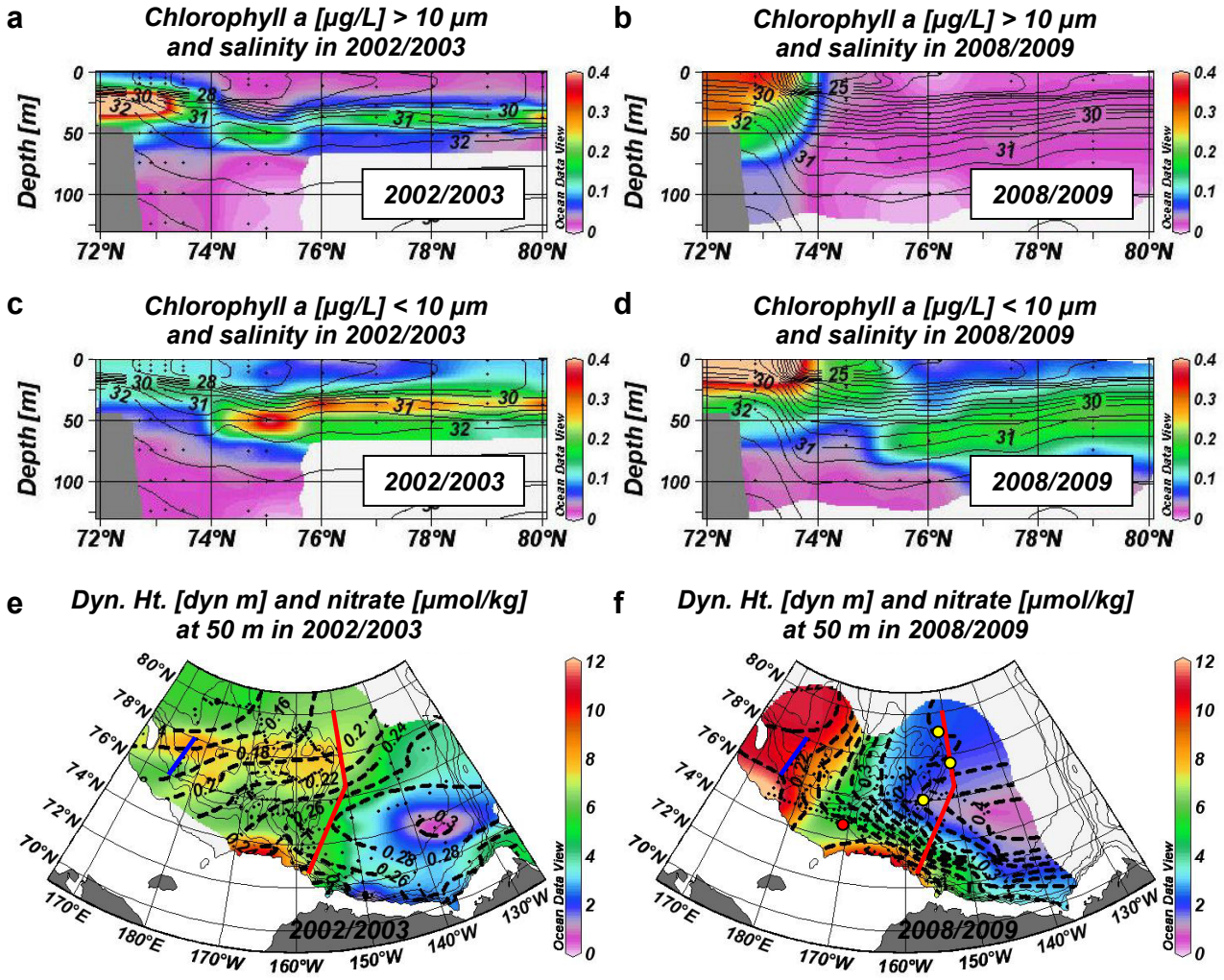

Fig. 2. Nishino *et al*.

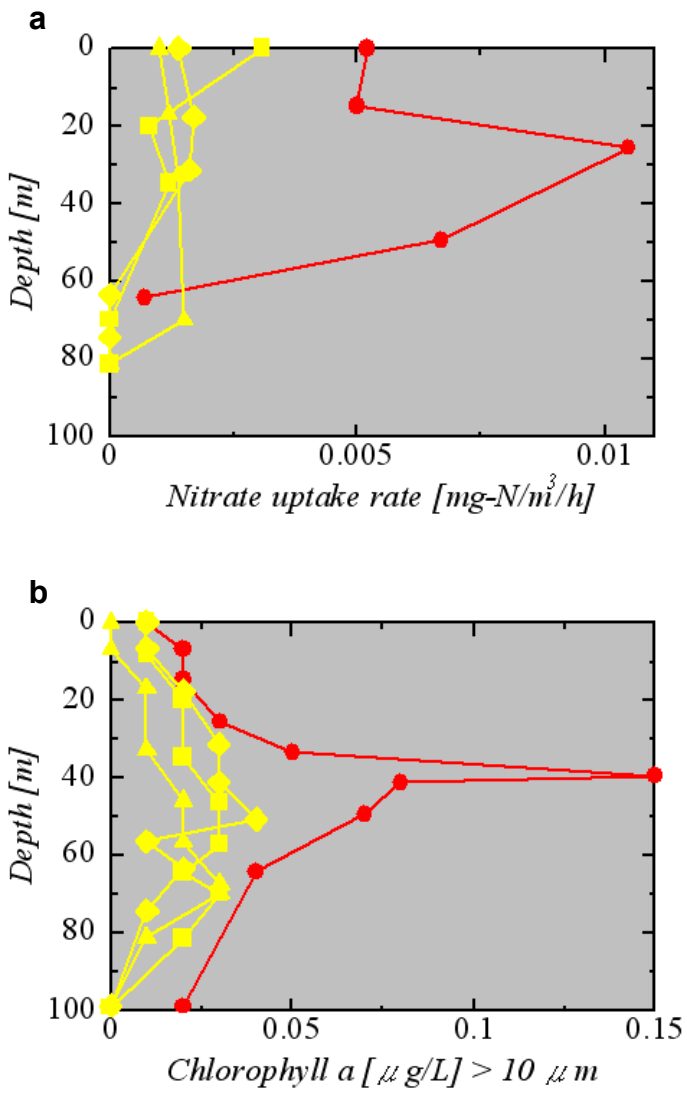

Fig. 3. Nishino *et al.*

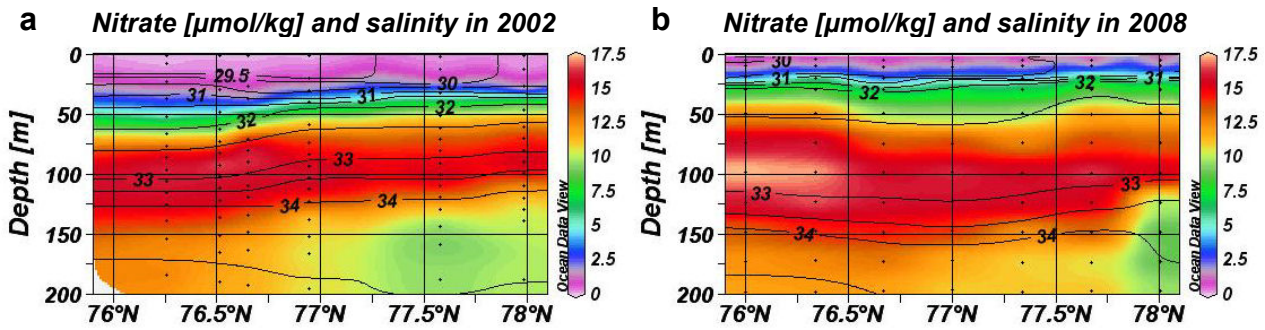

Fig. 4. Nishino *et al*.

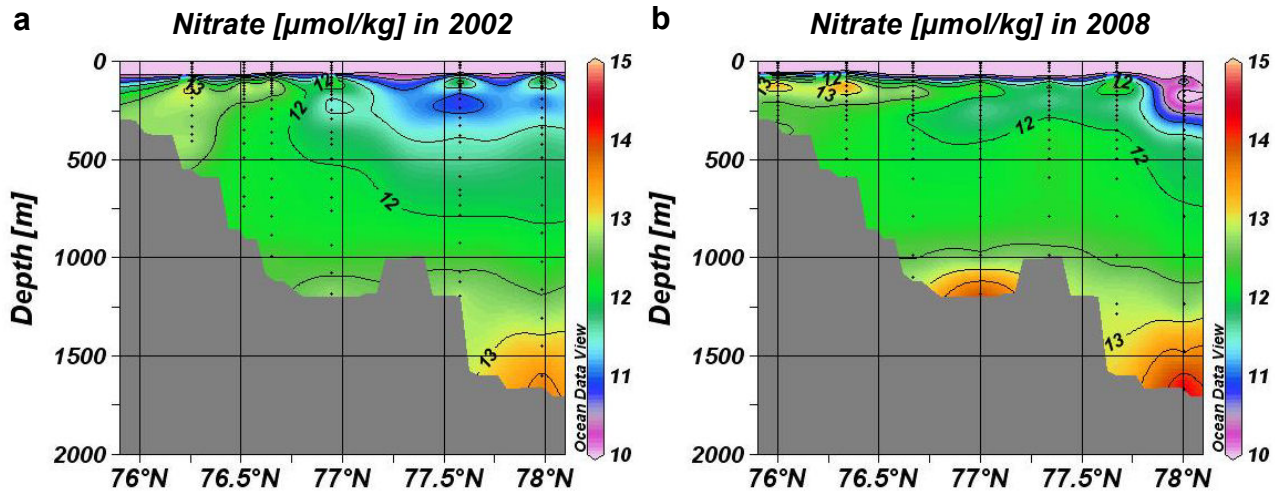

Fig. 5. Nishino *et al*.

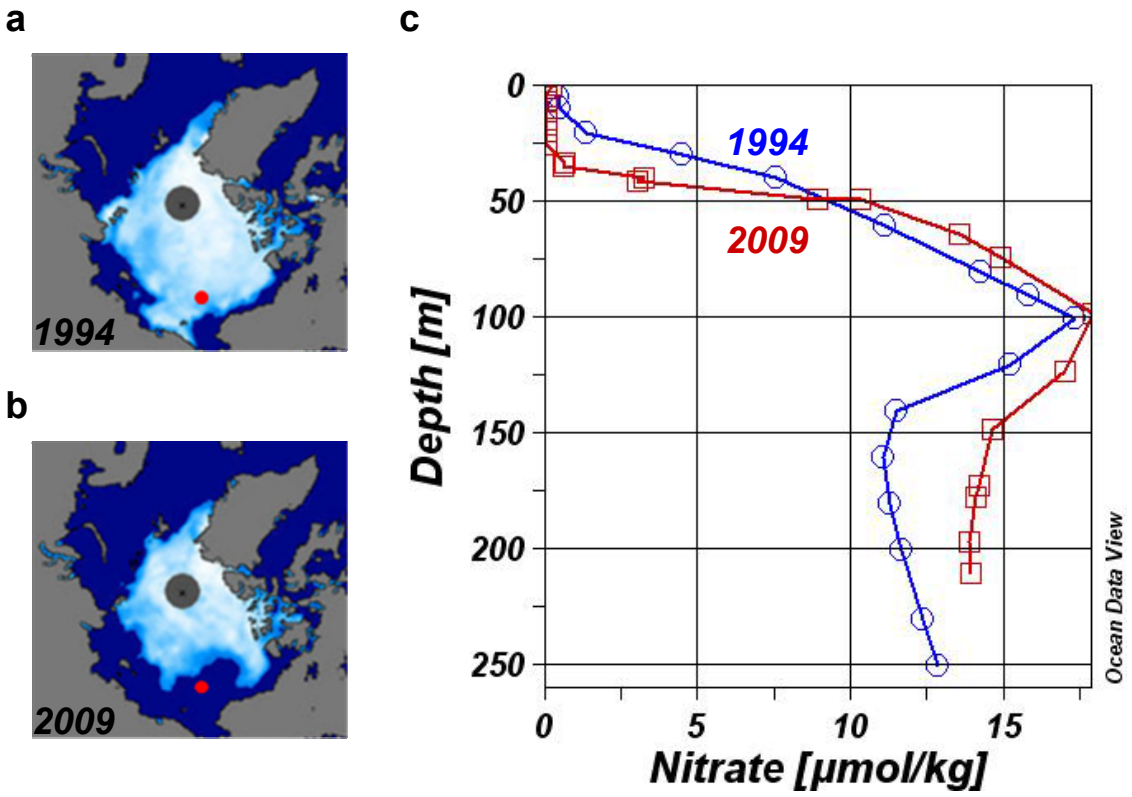

Fig. 6. Nishino *et al*.

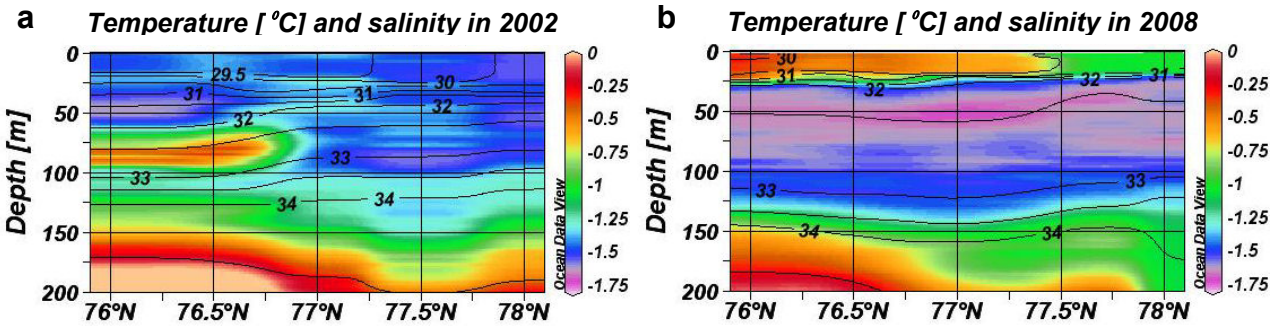

Fig. 7. Nishino *et al*.

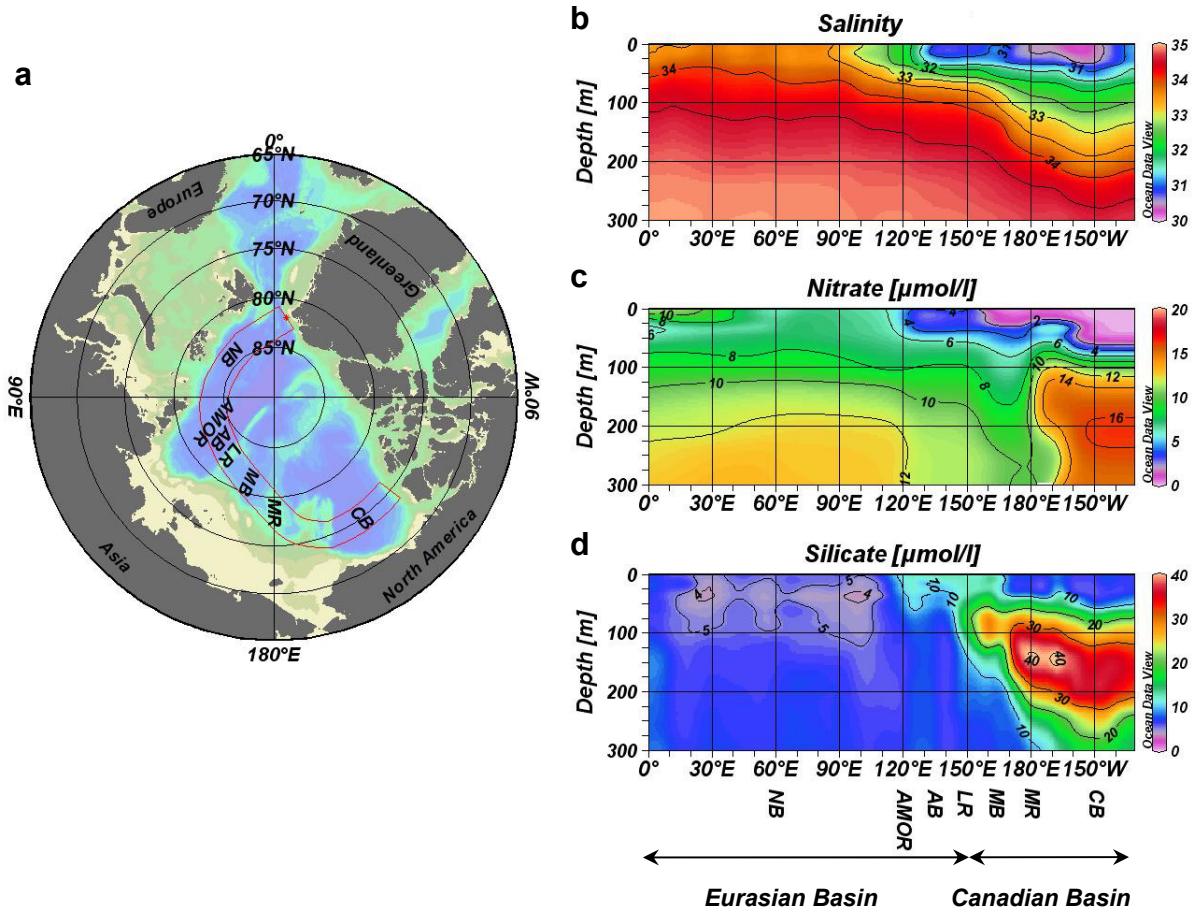

Fig. 8. Nishino *et al*.

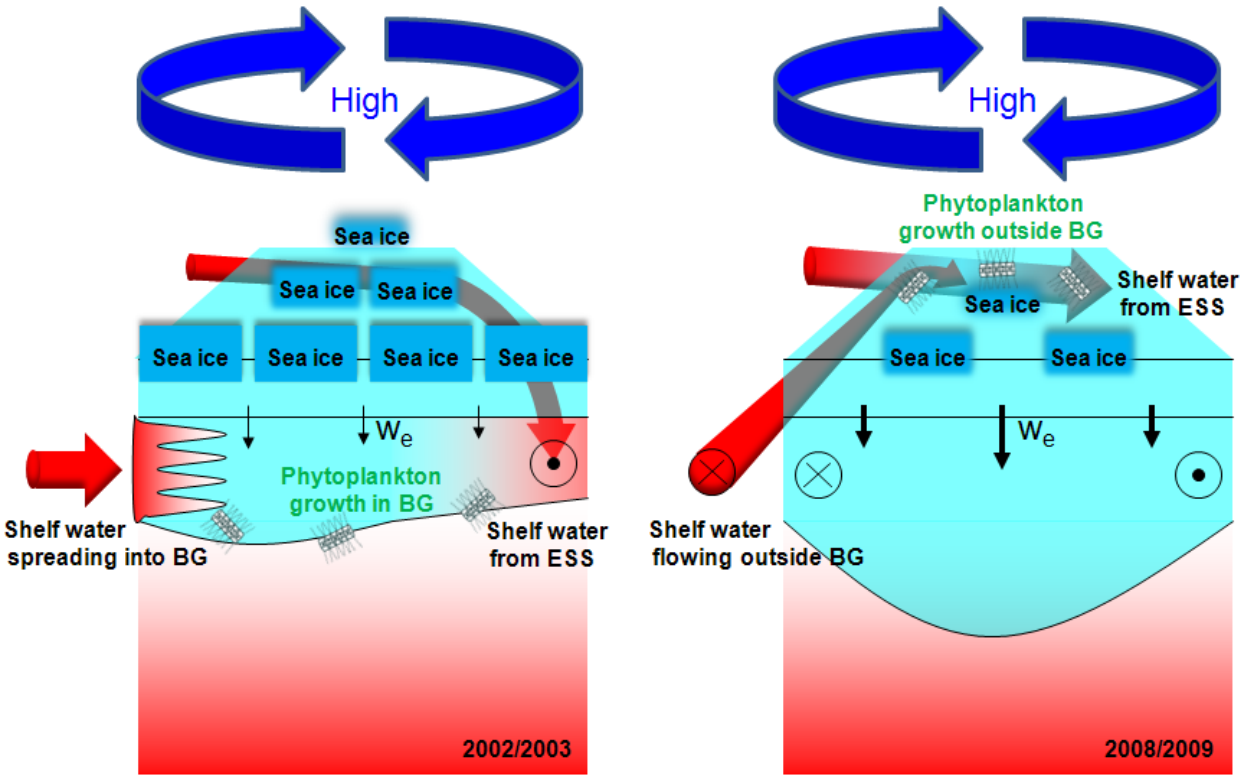

Fig. 9. Nishino *et al.*